University of Wollongong

Research Online

1-1-2016

Nanodroplets for stretchable superconducting circuits

Long Ren
University of Wollongong, lr289@uowmail.edu.au

Jincheng Zhuang
University of Wollongong, jincheng@uow.edu.au

Gilberto Casillas
University of Wollongong, gilberto@uow.edu.au

Haifeng Feng
University of Wollongong, hf533@uowmail.edu.au

Yuqing Liu
University of Wollongong, yl037@uowmail.edu.au

See next page for additional authors

Follow this and additional works at: https://ro.uow.edu.au/aiimpapers

Part of the Engineering Commons, and the Physical Sciences and Mathematics Commons

Recommended Citation

Nanodroplets for stretchable superconducting circuits

Abstract

The prospective utilization of nanoscale superconductors as micro/nanocoils or circuits with superior current density and no electrical resistance loss in next-generation electronics or electromagnetic equipment represents a fascinating opportunity for new microsystem technologies. Here, a family of superconducting liquid metals (Ga-In-Sn alloys) and their nanodroplets toward printable and stretchable superconducting micro/nanoelectronics is developed. By tuning the composition of liquid metals the highest superconducting critical temperature (Tc) in this family can be modulated and achieved as high as 6.6 K. The liquid metal nanodroplets retain their bulk superconducting properties and can be easily dispersed in different solvents as inks. The printable and stretchable superconducting micro/nano coils, circuits and electrodes have been fabricated by inkjet printer or laser etching by using superconducting nanodroplets inks. This novel superconducting system greatly promotes the commercial utilization of superconductors into advanced flexible micro/nanoelectronic devices and offers a new platform for developing more application with superconductors.

Keywords

circuits, superconducting, stretchable, nanodroplets

Disciplines

Engineering | Physical Sciences and Mathematics

Publication Details

Authors

Long Ren, Jincheng Zhuang, Gilberto Casillas, Haifeng Feng, Yuqing Liu, Xun Xu, Yundan Liu, Jun Chen, Yi Du, Lei Jiang, and Shi Xue Dou

Nano-droplets for Stretchable Superconducting Circuits

Long Ren, *Jincheng Zhuang*, *Gilberto Casillas*, *Haifeng Feng*, *Yuqing Liu*, *Xun Xu*,* *Yundan Liu*, *Jun Chen*, *Yi Du*,* *Lei Jiang*,* and *Shi Xue Dou*

L. Ren, [+] Dr. J. C. Zhuang, [+] H. F. Feng, Dr. X. Xu, Y. D. Liu, Dr. Y. Du, Prof. S. X. Dou
Institute for Superconducting and Electronic Materials
University of Wollongong
Wollongong, NSW 2500, Australia
E-mail: xun@uow.edu.au; yi_du@uow.edu.au

Dr. G. Casillas
Electron Microscopy Center
University of Wollongong
Wollongong, NSW 2500, Australia

Y. Q. Liu, Dr. J. Chen
Intelligent Polymer Research Institute and ARC Centre of Excellence for Electromaterials
Science
University of Wollongong
Wollongong, NSW 2500, Australia

Y. D. Liu
Laboratory for Quantum Engineering and Micro-Nano Energy Technology
School of Physics and Optoelectronics
Xiangtan University
Hunan 411105, China

Prof. L. Jiang
Key Laboratory of Bio-Inspired Smart Interfacial Science and Technology of the Ministry of
Education
School of Chemistry and Environment
Beihang University
Beijing 100191, China
E-mail: jianglei@iccas.ac.cn

[+] These authors contributed equally to this work.

1

1   Abstract: The prospective utilization of nanoscale superconductors as micro/nano coils or

2   circuits with superior current density and no electrical resistive loss in next-generation

3   electronics or electromagnetic equipment represents a fascinating opportunity for new

4   microsystem technologies. Here, we developed a family of superconducting liquid metals

5   (Ga-In-Sn alloys) and their nanodroplets toward printable and stretchable superconducting

6   micro/nanoelectronics. By tuning the composition of liquid metals, the highest

7   superconducting critical temperature (T_c) in this family can be modulated and achieved as

8   high as 6.6 K. The liquid metal nanodroplets retain their bulk superconducting properties, and

9   can be easily dispersed in different solvents as inks. The printable and stretchable

10   superconducting micro/nano coils, circuits and electrodes have been fabricated by inkjet

11   printer or laser etching by using superconducting nanodroplets inks. This novel

12   superconducting system greatly promotes the commercial utilization of superconductors into

13   advanced flexible micro/nano electronic devices, and offers a new platform for developing

14   more application with superconductors.

15
16   **1. Introduction**

17   Nanoscale superconductors, which are featured by high current transport density with no loss

18   and strong quantum-size oscillations effect below their critical temperature (T_c), have

19   attracted considerable attentions for building high-speed micro-/nano-electronic devices,

20   including rapid responding biosensor, quantum computer and micro Nuclear Magnetic

21   Resonance (NMR) device.[1-6] In despite of some recent progress on developing nano-sized

22   superconducting electronics by nanolithography techniques, the processing complexity and

23   high manufacture cost limit these superconducting micro/nanodevices in certain areas but not

24   practical in more extensive applications.[7-10] Moreover, the intrinsic brittleness of these

25   superconducting nanodevices does not allow any deformations, *e. g.* stretching or bending,

26   which make them impossible to be incorporated in flexible electronics.[11] Among all the

2

1 superconductors, Ga and Hg are exceptional which were expected to be used for

2 superconducting micro/nano devices because their room-temperature (RT) fluidity benefits

3 device processing and offers the devices RT-flexibility.[12-14] However, either low T_c (1.08 K

4 for Ga) less than liquid helium temperature (4.2 K, the lowest temperature for practical

5 application) or toxicity (Hg) of these two RT liquid metals (LM) significantly limits their

6 potential usage. To date, it is still a great challenge to develop superconductors that have a

7 comprehensive properties of non-toxicity, higher T_c, RT-fluidity/tractability, and good

8 wettability, which are highly demanded for the development of flexible superconducting

9 micro/nano electronics.

10   In this work, we developed a series of eutectic Gallium-Indium-Tin (EGaInSn) LMs and

11 corresponding nanodroplets (NDs), which can be used to fabricate flexible superconducting

12 micro/nanoelectronics by direct printing. These EGaInSn LMs demonstrate a great potential

13 for building flexible micro/nano electronics, owing to the RT fluidity, low resistivity, low

14 viscosity, and tractability of LMs.[15-18] More importantly, the intrinsic passivation of Ga

15 provides a solid oxide shell which replaces the original high-energy interface between metal

16 and outside, and ensures LM nanodroplets can keep excellent mechanical and electronic

17 properties of their bulk even when they are dispersed into solutions as the inks.[19-21] By

18 varying component proportions of Ga, In, and Sn in EGaInSn LMs, we have successfully

19 modulated superconducting T_c as high as 6.6 K. The EGaInSn NDs (~110 nm in diameter)

20 have also been prepared by an ultrasonication approach. These NDs retain their bulk

21 superconducting properties and can be dispersed and stored in various solvents, including

22 ethanol, acetone, and water. The EGaInSn ND dispersions exhibit excellent wettability to

23 metallic, oxide, and polymer surfaces. By using these dispersions as inks, stretchable and

24 flexible superconductive devices, including microsize superconducting coils, electric circuits,

25 and superconducting electrodes, have been fabricated and demonstrated on polyethylene

26 terephthalate (PET) and polydimethylsiloxane (PDMS) by direct printing and laser etching.

2. Results and Discussion

2.1. Formation and Characterization of the EGaInSn Nanodroplets.

The EGaInSn bulk alloy used here is a low-viscosity liquid at RT, with a composition of Ga, In, and Sn in different weight ratios. EGaInSn normally presents as millimeter-size droplets when dropped on a substrate under gravity.[22] These oval-shaped droplets can remain mechanically stabilized by intrinsic passivation due to the formation of a thin gallium oxide skin in air. Nevertheless, the skin obstructs direct printing of the Ga-based LMs in three-dimensional (3D) or two-dimensional (2D) structures with defined size.[23,24] For facilitating the printing of micro/nano-electronics, the EGaInSn NDs were obtained here via a simple ultrasonication process in the presence of thiols. In the typical synthesis, as shown in **Figure 1**(a), a certain amount of EGaInSn bulk was firstly dropped into an ethanolic solution of thiol. Then, probe sonication was applied to introduce cavitation in the solution, leading to local extremes of pressure and temperature for ultra-short life-spans. During this sonication, the liquid EGaInSn bulk stabilized by the oxidation layer was easily fractured under the oscillating shear force, and small LM droplets successively separated from the bulk matrix in a spherical shape, due to the high surface energy of the freshly exposed oxide-free surface.[25] In the meantime, thiolated ligands, which can easily and strongly bind to soft elements, readily assembled onto the surface of the new-born small EGaInSn droplets, competing with the re-oxidation process, which also took place at the interface.[20,26] Finally, spherical EGaInSn NDs (TEM image in Figure 1(a)) formed under continuous ultrasonication and remained mechanically stabilized because the protection from the thiolate-ligand self-assembly and rapid oxidation on the surface. After the ultrasonication and removal of excess thiols by washing with ethanol, grey slurry was obtained and redispersed in different solvents, which all remained suspended up to several weeks (see Figure S1, Supporting Information). The field-emission scanning electron microscope (FE-SEM) image in Figure 1(b) also

confirms that a large quantity of uniform spherical EGaInSn NDs was successfully

synthesized by the ultrasonication process. The particle size distribution of the samples

(Figure 1(c)) obtained after a 60 min sonication indicates an average diameter of about 110

nm.

Transmission electron microscope (TEM) together with energy dispersive X-ray (EDX)

elemental mapping of particles taken from the as-prepared EGaInSn (65% Ga, 24 % In, 11%

Sn by weight) suspension revealed the microstructure and constitution of the EGaInSn NDs

after ultrasonication. As seen in **Figure 2**(a) and (b), smooth core-shell-like spherical NDs are

uniformly packed together, and two concentric layers are evenly coated on the core. Despite

the slight size disparity among the different NDs, the inner and outer shells of these particles

are all ~ 3 nm thick and ~ 2 nm thick, respectively. Both the shells and the core are entirely

amorphous, which is similar to the case of the EGaInSn bulk sample at RT. The low

magnification high-angle annular dark field (HAADF) scanning TEM (STEM) images which

are sensitive to atomic number,[27] as well as the element mapping of the sample (Figure 2(c))

further verified that the amorphous NDs present a homogenous distribution of elements and

the element compositions of these NDs were the same as for the bulk. As proposed in the

schematic illustration of the synthetic process and confirmed by the EDX quantitative analysis

(Figure S2, Supporting Information), Ga, In, and Sn appear to be evenly dispersed in the core

of the ND in the same weight proportions as in the EGaInSn bulk sample. Oxygen and Ga are

present in the inner shell, and carbon is only present on the outer surface of the spherical ND.

The element mapping results confirmed that Ga is easily passivated to form an oxidation layer

when the nanosized EGaInSn drops are separated from the EGaInSn matrix and exposed in an

oxygen-rich environment. At the same time, an organic coating containing carbon surrounds

the gallium oxide during the thiolated ligand self-assembly process in the ethanol solution.

These two layers, as a result of the competition between thiolated ligand self-assembly and

the oxidation process, act as protective shells for the newborn EGaInSn NDs, which ensure

1   that these nanosized droplets are mechanically stabilized against coalescence in a neutral

2   solution or in the atmosphere. Akin to non-infiltration liquid droplets, these non-crystallized

3   EGaInSn NDs exhibit good elasticity and can deform under the pressure of other particles

4   (Figure 2(a)), due to the liquid characteristic of the core and the protection of the hetero-phase

5   shells.

6   **2.2. Temperature dependence crystallization property of the EGaInSn nanoparticles.**

7

8   Nanomaterials exhibit exotic physical properties, in contrast to their bulk forms, due to the

9   size effect. Generally, the melting points of metals are depressed in nanomaterials.[28-30]

10   Determination of the crystallization behavior of EGaInSn NDs is therefore critical for

11   processing micro/nano devices. In-situ temperature-dependent TEM was applied here in order

12   to determine the melting point and to investigate the crystallization process for the as-

13   prepared EGaInSn NDs. As shown in Figure 2(d) and in Supporting Information Figures S3

14   and S4, snapshot TEM images and selected area electron diffraction (SAED) patterns of

15   EGaInSn NDs were recorded every 10 °C (10 K) from RT to liquid nitrogen temperature (77

16   K). The crystallization of EGaInSn occurs at −80 °C (193 K), as the corresponding SAED

17   pattern shows well-defined diffraction spots. While the spots in the pattern were clear, they

18   appeared and disappeared in a time frame of seconds, which is due to spontaneous

19   amorphization and recrystallization at this temperature. Interestingly, the NDs undergo a

20   phase separation accompanied by crystallization. It is clearly demonstrated in high-resolution

21   TEM (HRTEM) images that a small part of each individual ND has separated out from the

22   amorphous matrix. The SAED patterns indicate that these separated parts only consist of In

23   and Sn (see details in the corresponding SAED pattern information in Figure S4, Supporting

24   Information). With further cooling, the crystallized Ga appeared at the temperature of

25   −140 °C (133 K). Moreover, the SAED pattern of the NDs was retained and did not change

26   any more with further decreasing temperature, indicating the fully crystalline state of all the

6

1 EGaInSn NDs. The HAADF image and element mapping of these NDs further confirmed the

2 phase separation during this cooling process. These results imply that the melting point or the

3 fully crystalline point from liquid to solid of the as-prepared EGaInSn NDs was ~ −140 °C

4 (133 K, defined as T^*), which is depressed by almost 150 °C (150 K) compared with the bulk

5 EGaInSn (~10 °C, 283 K).

6

7 **2.3. Mechanical and electricity properties of the EGaInSn nanoparticles and EGaInSn-**
8 **NP-based printed electronics..**

9

10 After the nanosizing process, the uniform ethanol dispersion of EGaInSn NDs enables easy

11 fabrication of fine microcircuits and functional devices by inkjet printing, laser lithography,

12 and even handwriting. As demonstrated in **Figure 3** and the Supporting Information (Video

13 S1, Supporting Information), different microsized RT-flexible devices on PET and PDMS

14 substrates, including planar coils and electrode arrays, were fabricated by inkjet printing

15 and/or laser lithography. Generally, printed flexible devices suffer from low conductivity

16 because of the poor in-plane electrical connections between NDs with

17 insulating/semiconducting shell structures.[31,32] Unlike the conventional solid metallic or

18 conductive polymer NDs, which need various complicated sintering methods to improve their

19 conductivity in printed devices, the in-plane electrical conductivity of EGaInSn NDs films can

20 be enhanced by a facile 'mechanical sintering' method.[33-36] In other words, the insulating

21 shells of the EGaInSn NDs can be easily broken by external force, and thus, the electrical

22 connections can be significantly improved by merging individual NDs together. We

23 quantified the breakthrough of an individual EGaInSn ND (~ 100 nm in diameter) under

24 external force by an atomic force microscope (AFM) force-displacement measurement

25 (Figure 3(a)). First, the AFM tip was made to approach the individual EGaInSn ND until

26 negative force feedback was observed (indicating attraction between the tip and the ND

surface due to van der Waals attraction). The tip was then lowered to touch the ND surface by

further reducing the tip-sample distance. After that, a gradually increasing force was applied

to the surface through the tip, which led to the compressive deformation of the ND, as

reflected by the linear force-displacement behavior. When the applied force was greater than

~ 50 nN, breakthrough of the EGaInSn ND occurred, as evidenced by the kink that appears in

the force-displacement curve. In the retraction process (shown by the blue curve), the force

curve does not overlap with the curve corresponding to the approaching force curve (in red).

This is attributed to the adhesion between the tip and the liquid core of the ND, as well as the

great surface tension of EGaInSn. The I-V curves before and after the breaking of the

EGaInSn ND by external pressure (the process called 'mechanical sintering') were also

measured by using the AFM conductive mode (c-AFM). Excellent electrical conductivity was

achieved in the individual ND after the shell breaking, indicating that nanosized EGaInSn

droplets also retain the same high electrical conductivity as the bulk form. The EGaInSn

flexible electric circuits on PDMS can retain high in-plane conductivity after a hundred

rounds of bending and folding (Figure 3(b)). This illustrates that the mechanical sintering

process is easily conducted to realize the coalescence of EGaInSn NDs, and hence, that the

electrical conductivity of the EGaInSn-ND-based flexible circuits can be greatly improved.

2.4. Superconductivity of the EGaInSn nanoparticles and EGaInSn-NP-based printed electronics.

Having demonstrated the good electrical conductivity of the microelectronics printed by the

as-prepared EGaInSn NDs, the superconductivity of the EGaInSn alloy at low temperature is

now first revealed in this work. The transition temperature of EGaInSn can be modulated by

varying the ratio of its component elements, as shown in Figure S6 and Table S1 (Supporting

Information). The EGaInSn sample with the highest T_c among all the samples was

8

1   $Ga_{30}In_{47}Sn_{23}$ (30% Ga, 47 % In, 23% Sn by weight), the T_c of which reaches as high as 6.6 K,

2   which is much higher than those of the individual components (1.08 K for Ga, 3.41 K for In,

3   and 3.73 K for Sn).[37,38] This transition temperature is above the liquefaction point of helium,

4   promoting this alloy's practical application. Thus, the $Ga_{30}In_{47}Sn_{23}$ in the forms of bulk alloy

5   and NDs was chosen to study the superconducting properties. **Figure 4**(a) displays a

6   comparative study of the temperature dependence of the resistivity (ρ-T) between the

7   $EGa_{30}In_{47}Sn_{23}$ bulk sample and an $EGa_{30}In_{47}Sn_{23}$-ND-based printed circuit, which show

8   similar metallic behavior above 6.6 K. It was found that the conductivities of the bulk and ND

9   liquid metal samples show a slight difference at room temperature but almost the same below

10 T_C. It should note that there is a jump in ρ-T curves at around 225 K for both bulk and ND

11 samples. Considering that the value of 225 K is close to phase separation and crystallization

12 temperature observed in TEM characterizations, the origin of this jump is most likely

13 attributed to effect of the transition from amorphous matrix to crystallized samples in this

14 system. In this case, the scattering for charge carriers is significantly depressed due to the

15 formation of long-range ordered phonon vibration, leading to cliffy increase in conductivity,

16 *i.e.*, an obvious dip in temperature dependent resistivity. The inset of Figure 4(a) shows an

17 enlarged view of the ρ-T curve at low temperature, ranging from 2 K to 8 K, where the two

18 samples demonstrate the same superconducting transition at the temperature of 6.6 K. The

19 enhancement of the T_c compared to the individual components of the alloy is confirmed by

20 the temperature dependence of the zero-field-cooled (ZFC) and field-cooled (FC)

21 magnetization measurements at 50 Oe for the $EGa_{30}In_{47}Sn_{23}$ bulk sample and the

22 $EGa_{30}In_{47}Sn_{23}$ ND sample, as shown in Figure 4(b). Both the transport measurements and the

23 magnetic measurements imply that the superconducting properties of EGaInSn have scarcely

24 degenerated after nano-crystallization. More importantly, as a flexible printed device, the

25 $EGa_{30}In_{47}Sn_{23}$-ND-based printed circuit can be deformed to be any shape in RT and retain the

26 superconducting properties without any fading. (See Figure S7, Video S2 and Video S3,

Supporting Information) It should be noted that the diameter of nanoparticles is crucial for retaining the superconductivity, since the coherence length (ξ) is also on the nanometer scale. In superconductivity, ξ is the characteristic exponent of variation of the range of the superconducting order parameter, which is related to the Cooper pair size in the Bardeen-Cooper-Schrieffer (BCS) theory.[1] The superconducting order parameter could be strongly suppressed in the vicinity of a structural defect, such as a grain boundary in our case, with the effective size comparable to the coherence length ξ, leading to the destruction of the superconductivity. The EGaInSn NDs here retain their superconducting properties under the condition that their diameter is at least twice as large as the superconducting coherence length ξ. Thus, the diamagnetic signal of the ND sample is contributed by the magnetic moment residing in the NDs under magnetic field. Along with the crystalline state at low temperature of the ND sample shown in Figure 2(d), three temperature regions were defined, as shown in the inset of Figure 4(b). When T > T^* (fully crystalline temperature point of EGaInSn NDs), the three kinds of atoms (Ga, In, Sn) are in the amorphous state, and magnetic field directly penetrates the ND without generating a magnetic moment. For the region T_c < T < T^*, the three kinds of atoms are arranged in an ordered structure, leading to crystalline NDs. Nevertheless, there is still no magnetic moment, because the temperature is higher than T_c. The NDs enter into the superconducting state for T < T_c, in which the perfect diamagnetism expels the field from the interior of the NDs.

Due to their rigidity and bad connectivity, high temperature superconductors, such as MgB_2, pnictides, and cuprates, are extremely difficult to incorporate into flexible micro/nano-devices.[11] The enhancement of T_c in the EGaInSn alloy above the liquid helium critical point (4.2 K) paves the way for this flexible material to become a practical candidate for micro/nano superconducting electronics. Moreover, their non-toxic nature allows EGaInSn alloys and their NDs to be practically and safely used for flexible, low-cost, and lightweight

micro/nano electronic devices, including, but not limited to, energy devices, microelectromechanical systems (MEMS), NMR, sensors and display devices.

3. Conclusion

In this work, a series of EGaInSn alloys and their corresponding nanosized droplets with different weight ratios of the component elements have been developed for realizing stretchable and printable superconductor microcircuits. We have employed sonication and thiol self-assembly to successfully prepare EGaInSn NDs with average particle sizes of ~ 110 nm. A systematic characterization of the microstructure, crystallization, phase changes, and mechanical properties was carried out on the as-prepared EGaInSn NDs. The crystallization and phase separation of these EGaInSn NDs take place as the temperature decreases from RT to liquid nitrogen temperature. Their applicability to inkjet printing, laser lithography, and handwriting to create different patterns is shown here to demonstrate their suitability for flexible superconducting microcircuits. Finally, the superconductive properties of such circuits based on the EGaInSn NDs with different weight ratios are also analyzed. These discoveries provide strong prospects for the EGaInSn NDs as promising candidates for developing practical stretchable superconducting micro/nano devices. Moreover, this novel superconducting system has a huge potential to be extended with other metal, which offers a new platform for developing more application with superconductors.

4. Experimental Section

Preparation of EGaInSn Bulk and Nanodroplets: EGaInSn bulk samples with various component proportions were prepared by co-melting Ga, In, and Sn in the appropriate weight ratio. For typical EGaInSn nanodroplets preparation, 1 g bulk GaInSn alloy was added into 100 mL ethanol solution containing 0.5 mg ethyl 3-mercaptopropionate. Then, ultrasonication was performed using a conical tip sonicator (Sonics VCX 750 ultrasonic processor, with a 19 mm diameter high-gain solid probe) in this solution. The power of the ultrasonication was

directly controlled by the instrument as 40 % of the maximum power (750 W), the amplitude of the sonicator was adjusted to 80 %, and the sonication proceeded for 60 minutes. The temperature of the sample during ultrasonication was controlled by using a cold water bath at about 20 °C. After sonication, the slurry was further washed by neat ethanol several times, followed by mild centrifugation to remove the excess thiol, and then the samples were suspended and stored in neat ethanol for further use.

Morphology Characterization: Field-emission scanning electron microscopy (FE-SEM) observations were performed using a JEOL JSM-7500FA microscope. Samples for FE-SEM characterization were prepared by depositing EGaInSn suspension onto Si wafers. The diameters of the as-prepared nanoparticles were obtained by counting more than 200 particles in several SEM micrographs for each sample, using the ImageJ free software. Transmission electron microscope (TEM) images, SAED patterns, HAADF images and STEM-EDX spectra were obtained using a JEOL ARM-200F and a Tecnal G2 F20 operating at 200 kV with an EDAX solid-state X-ray detector.

In-situ Temperature TEM Analysis: A TEM Cu grid with EGaInSn nanodroplets was loaded into a liquid nitrogen cooling holder from JEOL. Temperature control of the specimen was achieved through a metallic rod connecting the specimen holder to the liquid nitrogen dewar, which contains an electric heater for heating and adjusting the temperature. The TEM images and SAED patterns were collected every 10 °C from RT using a JEOL ARM-200F operated at 200 kV. The HAADF images were collected using a 50 mrad inner collection angle and a 180 mrad outer collection angle. The STEM-EDX spectrum was acquired by a NORAN SDD with a ~1 sr collection angle, at −150 °C.

Atomic Force Spectroscopy (AFM) Measurements: The force-displacement measurements were performed in air using a JPK Nanowizard AFM. 28 nm diameter silicon based tips with frequency of 70 kHz and spring constant of 2 N/m were used to apply a 36 nN force on an individual EGaInSn nanodroplet for the force spectra. The I-V curves before and after

breaking the EGaInSn nanodroplets with the tip were also collected by using the AFM conductive mode (c-AFM). Both force and conductive analysis was performed in contact mode.

Fabrication of Micro-Patterns or Electronics: The inkjet ink used for printing was a 200 mg/10 mL EGaInSn nanodroplets suspension in ethanol. The patterns were directly printed on a flexible plastic substrate (PET). For the patterns and electrodes prepared by laser lithography, a uniform thin film of the EGaInSn nanodroplets ethanol suspension was first deposited on PDMS elastomer. Then, a fiber laser cutter system (Universal PLS6MW Multi-Wavelength Laser Platform, 1.06 μm, 30 watts, spot size of ~25 μm) was used to etch the unwanted components and achieve the desired pattern and electrode. For EGaInSn thin-film etching, the laser power was set at 23%, the scan speed was fixed at 10% and image quality level was set as 'Quality'.The mechanical sintering route to make the conductive paths for micro-patterns or electrodes was conducted using a writing utensil to press the top surface of the plastic and PDMS. The resistance of these electrodes after the mechanical sintering process and continuous bending process was recorded by a multimeter.

Superconductivity and Magnetization Measurements: Resistivity was measured using a physical property measurement system (PPMS) with a standard four-probe method. Samples 2 mm × 5 mm × 0.1 mm in size were prepared for the resistivity measurement. DC magnetization and the magnetic relaxation measurements were performed using the vibrating sample magnetometer (VSM) option of the PPMS.

[1] M. Tinkham, *Introduction to superconductivity*, New York : McGraw Hill, **1996**.

[2] Y. Guo, Y.-F. Zhang, X.-Y. Bao, T.-Z. Han, Z. Tang, L.-X. Zhang, W.-G. Zhu, E. G. Wang, Q. Niu, Z. Q. Qiu, J.-F. Jia, Z.-X. Zhao, Q.-K. Xue, *Science* **2004**, *306*, 1915.

[3] C. Granata, A. Vettoliere, *Phys. Rep.* **2016**, *614*, 1.

[4] Y. Miyata, K. Nakayama, K. Sugawara, T. Sato, T. Takahashi, *Nat. Mater.* **2015**, *14*, 775.

[5] S. X. Dou, W. K. Yeoh, O. Shcherbakova, D. Wexler, Y. Li, Z. M. Ren, P. Munroe, S. K. Chen, K. S. Tan, B. A. Glowacki, J. L. MacManus-Driscoll, *Adv. Mater.* **2006**, *18*, 785.

[6] S. Ichinokura, K. Sugawara, A. Takayama, T. Takahashi, S. Hasegawa, *ACS Nano* **2016**, *10*, 2761.

[7] J. P. Cleuziou, WernsdorferW, BouchiatV, OndarcuhuT, MonthiouxM, *Nat. Nano.* **2006**, *1*, 53.

[8] S. Mandal, T. Bautze, O. A. Williams, C. Naud, É. Bustarret, F. Omnès, P. Rodière, T. Meunier, C. Bäuerle, L. Saminadayar, *ACS Nano* **2011**, *5*, 7144.

[9] T. Schwarz, J. Nagel, R. Wölbing, M. Kemmler, R. Kleiner, D. Koelle, *ACS Nano* **2013**, *7*, 844.

[10] K. Senapati, M. G. Blamire, Z. H. Barber, *Nat. Mater.* **2011**, *10*, 849.

[11] S. R. Foltyn, L. Civale, J. L. MacManus-Driscoll, Q. X. Jia, B. Maiorov, H. Wang, M. Maley, *Nat. Mater.* **2007**, *6*, 631.

[12] P. L. Richards, M. Tinkham, *Phys. Rev.* **1960**, *119*, 575.

[13] W. D. Gregory, *Phys. Rev.* **1968**, *165*, 556.

[14] R. W. Cohen, B. Abeles, G. S. Weisbarth, *Phys. Rev. Lett.* **1967**, *18*, 336.

1   [15]   R. C. Chiechi, E. A. Weiss, M. D. Dickey, G. M. Whitesides, *Angew. Chem. Int. Ed.*

2   **2008**, *47*, 142.

3   [16]   M. D. Dickey, R. C. Chiechi, R. J. Larsen, E. A. Weiss, D. A. Weitz, G. M.

4   Whitesides, *Adv. Funct. Mater.* **2008**, *18*, 1097.

5   [17]   L. Sheng, J. Zhang, J. Liu, *Adv. Mater.* **2014**, *26*, 6036.

6   [18]   R. K. Kramer, C. Majidi, R. J. Wood, *Adv. Funct. Mater.* **2013**, *23*, 5292.

7   [19]   M. R. Khan, C. B. Eaker, E. F. Bowden, M. D. Dickey, *Proc. Natl. Acad. Sci. U.S.A.*

8   **2014**, *111*, 14047.

9   [20]   A. Yamaguchi, Y. Mashima, T. Iyoda, *Angew. Chem. Int. Ed.* **2015**, *54*, 12809.

10   [21]   Y. Lu, Q. Hu, Y. Lin, D. B. Pacardo, C. Wang, W. Sun, F. S. Ligler, M. D. Dickey, Z.

11   Gu, *Nat. Commun.* **2015**, *6*, 10066.

12   [22]   T. Liu, P. Sen, C. J. Kim, *J. Microelectromech. Syst.* **2012**, *21*, 443.

13   [23]   C. Ladd, J.-H. So, J. Muth, M. D. Dickey, *Adv. Mater.* **2013**, *25*, 5081.

14   [24]   Y. Lin, C. Cooper, M. Wang, J. J. Adams, J. Genzer, M. D. Dickey, *Small* **2015**, *11*,

15   6397.

16   [25]   J. N. Hohman, M. Kim, G. A. Wadsworth, H. R. Bednar, J. Jiang, M. A. LeThai, P. S.

17   Weiss, *Nano Lett.* **2011**, *11*, 5104.

18   [26]   B. Pokroy, B. Aichmayer, A. S. Schenk, B. Haimov, S. H. Kang, P. Fratzl, J.

19   Aizenberg, *J. Am. Chem. Soc.* **2010**, *132*, 14355.

20   [27]   S. J. Pennycook, *Ultramicroscopy* **1989**, *30*, 58.

21   [28]   M. Takagi, *J. Phys. Soc. Jpn.* **1954**, *9*, 359.

22   [29]   M. Dippel, A. Maier, V. Gimple, H. Wider, W. E. Evenson, R. L. Rasera, G. Schatz,

23   *Phys. Rev. Lett.* **2001**, *87*, 095505.

24   [30]   A. Mataz, B. M. Gregory, *J. Phy. Condens. Matter* **2005**, *17*, R461.

25   [31]   S. Sivaramakrishnan, P.-J. Chia, Y.-C. Yeo, L.-L. Chua, P. K. H. Ho, *Nat. Mater.*
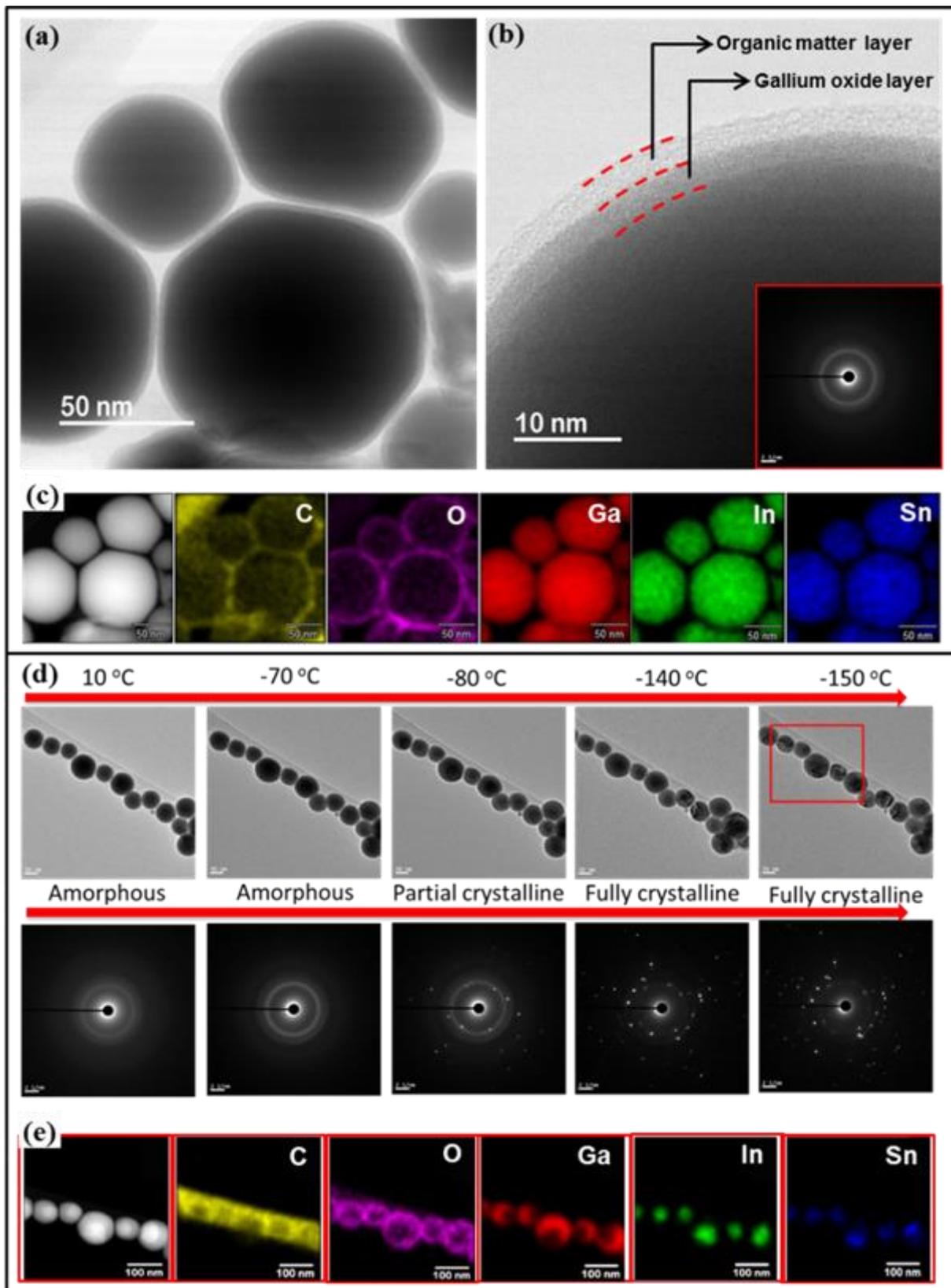
26   **2007**, *6*, 149.

1 [32] M. Grouchko, A. Kamyshny, C. F. Mihailescu, D. F. Anghel, S. Magdassi, *ACS Nano*

2   **2011**, *5*, 3354.

3 [33] B. Y. Ahn, E. B. Duoss, M. J. Motala, X. Guo, S.-I. Park, Y. Xiong, J. Yoon, R. G.

4   Nuzzo, J. A. Rogers, J. A. Lewis, *Science* **2009**, *323*, 1590.

5 [34] J. Perelaer, B. J. de Gans, U. S. Schubert, *Adv. Mater.* **2006**, *18*, 2101.

6 [35] S. B. Walker, J. A. Lewis, *J. Am. Chem. Soc.* **2012**, *134*, 1419.

7 [36] J. W. Boley, E. L. White, R. K. Kramer, *Adv. Mater.* **2015**, *27*, 2355.

8 [37] M. F. Merriam, M. Von Herzen, *Phys. Rev.* **1963**, *131*, 637.

9 [38] G. Knapp, M. F. Merriam, *Phys. Rev.* **1965**, *140*, A528.

10

Figure 1. (a) Schematic illustration of the preparation route for EGaInSn nanodroplets. Before ultrasonication, the EGaInSn bulk sample presents as millimeter sized droplets. After ultrasonication in the ethanolic solution of thiol, the millimeter droplets are separated into nanometer sized droplets. (b) FE-SEM image of EGaInSn nanodroplets prepared by 40 % power ultrasonication at 20 °C for 60 min. (c) Size distribution of EGaInSn nanodroplets. The mean diameter is ~110 nm.
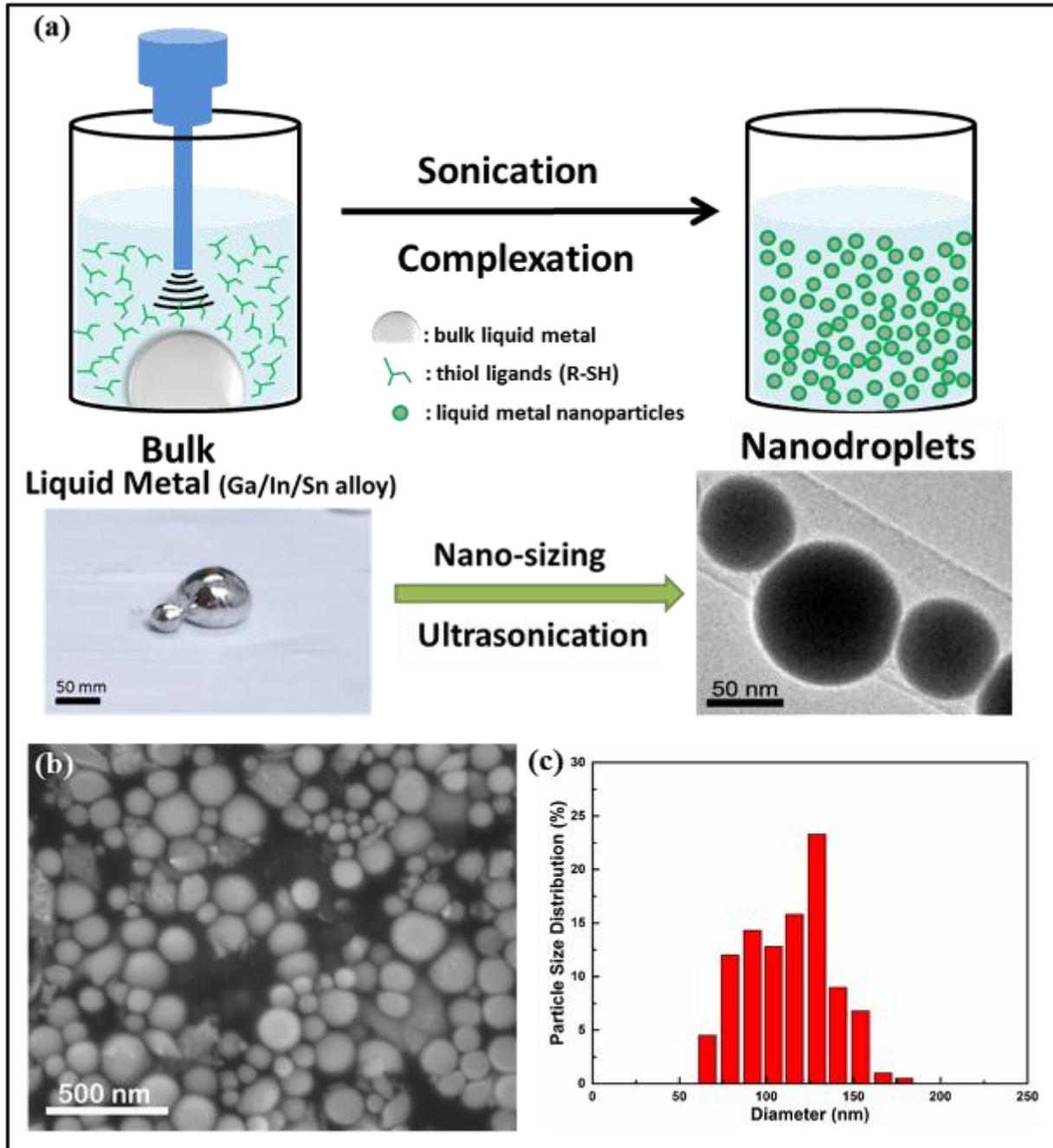
Figure 2. TEM and scanning TEM (STEM) characterization of EGaInSn nanodroplets at room temperature: (a) Representative TEM image of EGaInSn nanodroplets. (b) HRTEM image demonstrates the core-shell structure of EGaInSn nanodroplets; the black core is the liquid metal (EGaInSn alloy), and the lighter part is the coating shell; two layers of shell can be observed: the inner coating (gallium oxide) is ~ 3 nm thick, and the organic matter layer is ~ 3 nm; the inset is the corresponding selected area electron diffraction (SAED) pattern. (c) A typical STEM image of EGaInSn nanodroplets, as along with element mapping of the same EGaInSn nanodroplets. From left to right, the images shows EGaInSn nanodroplets mapped for C (yellow), O (magenta), Ga (red), In (green), and Sn (blue). TEM images at different temperatures of EGaInSn nanodroplets: (d) TEM images (top) and the corresponding SAED patterns (bottom) of EGaInSn nanodroplets at representative temperatures: from left to right, 10 °C (283 K), −70 °C (203 K), −80 °C (193 K), −140 °C (133 K), and −150 °C (123 K). (e) STEM image of EGaInSn nanodroplets, as along with element mapping of the same EGaInSn nanodroplets at −150 °C (123 K): from left to right, the images show EGaInSn nanodroplets and mappings for C (yellow), O (Magenta), Ga (red), In (green), and Sn (blue).

(a) 50 nm

(b) Organic matter layer
Gallium oxide layer
10 nm

(c) C | O | Ga | In | Sn

(d) 10 °C | -70 °C | -80 °C | -140 °C | -150 °C
Amorphous | Amorphous | Partial crystalline | Fully crystalline | Fully crystalline

(e) C | O | Ga | In | Sn

1
2
3
4

Figure 3. (a) Force–displacement curve obtained for one individual EGaInSn nanodroplet; the red line tracks the approach process between the AFM tip and the particle, while the blue line tracks the retraction of the AFM tip from the particle; the inset presents the I-V curves before and after the EGaInSn nanodroplet is broken by the applied external pressure. (b) The upper two images are digital images of sintered flexible circles printed with the EGaInSn nanodroplet based inkjet, and of the good electrical conductivity measured by a multimeter (inset of right panel). On the bottom left, a digital image shows a flexible microcoil and microgapped interdigitated electrode prepared by laser lithography from a EGaInSn nanodroplets film assembled on PDMS; on the bottom right, the resistance stability of the microcoil on PDMS after mechanical sintering is demonstrated over a hundred rounds of bending and folding.

20
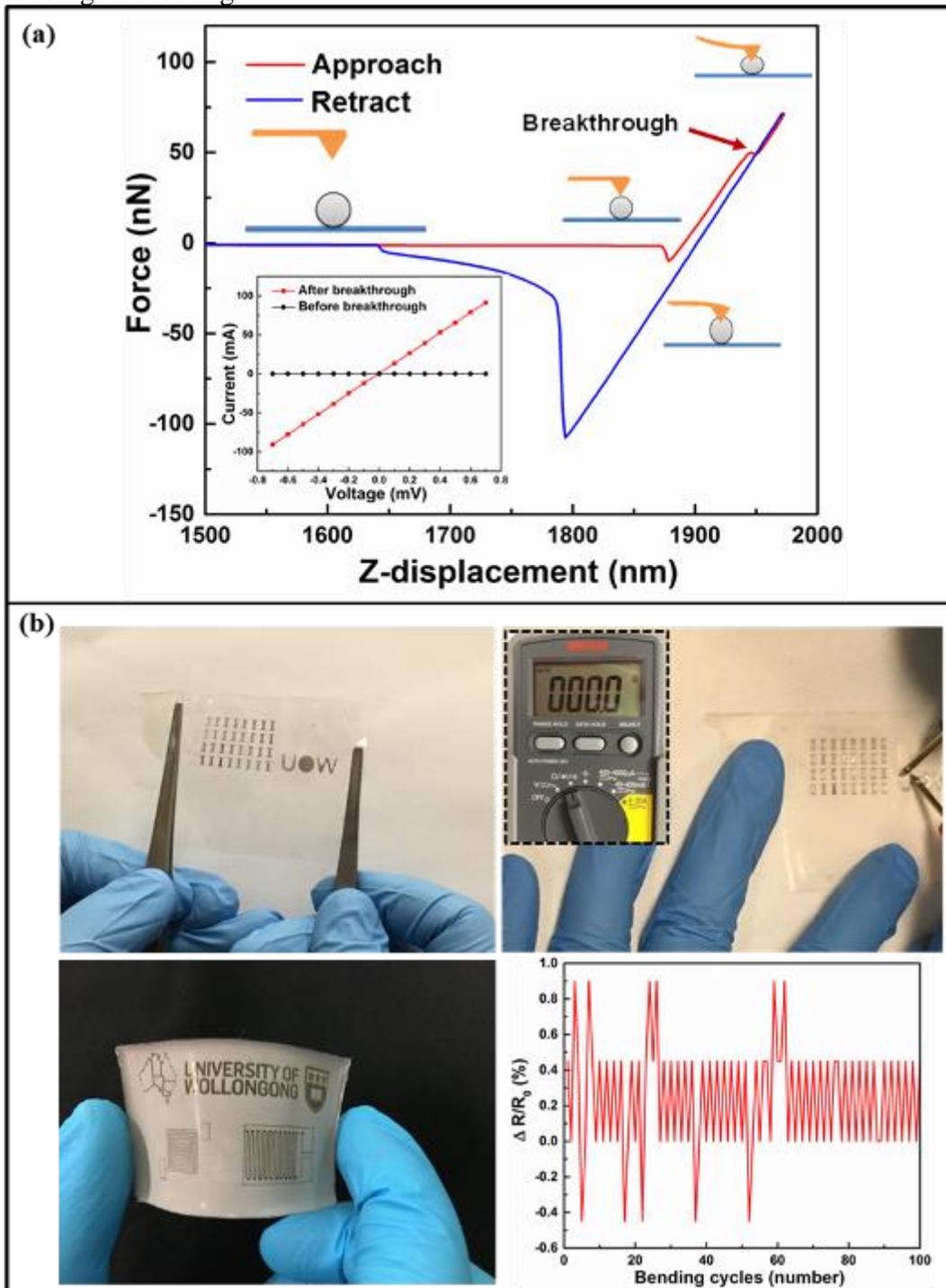
1　**Figure 4.** (a) Temperature dependence of the resistivity (ρ-T curves) between 2 K and 300 K
2　for the EGaInSn bulk sample (2 mm × 5 mm × 0.2 mm) and a printed EGaInSn nanodroplets
3　pattern (2 mm × 5 mm × 0.1 mm) after mechanical sintering; inset: enlargement of the ρ-T
4　curves between 2 K and 8 K. The superconducting transition temperatures Tc of these two
5　samples are both around 6.6 K. (b) Zero-field cooling and field cooling (ZFC, FC)
6　magnetization curves from 2 to 300 K of the EGaInSn nanodroplets under a magnetic field of
7　50 Oe. The inset schematic illustrations show that the EGaInSn nanodroplet would make the
8　transition to crystalline from amorphous as the temperature decreases from RT (300 K) to T*
9　(133 K, fully crystalline temperature point of EGaInSn NDs). The amorphous and then the
10　crystalline EGaInSn nanodroplet remains paramagnetic when the temperature is above the Tc
11　(~ 6.6 K), but the crystalline EGaInSn nanodroplet will change to diamagnetic when the
12　temperature falls below Tc (~ 6.6 K) due to the Meissner effect in the superconducting
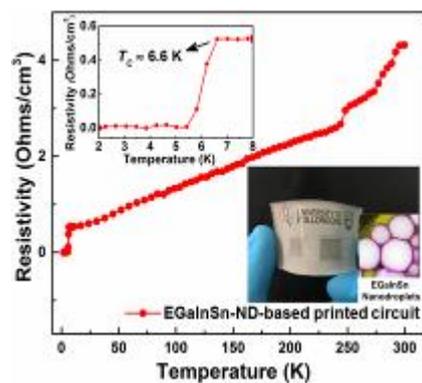13　EGaInSn nanodroplet.
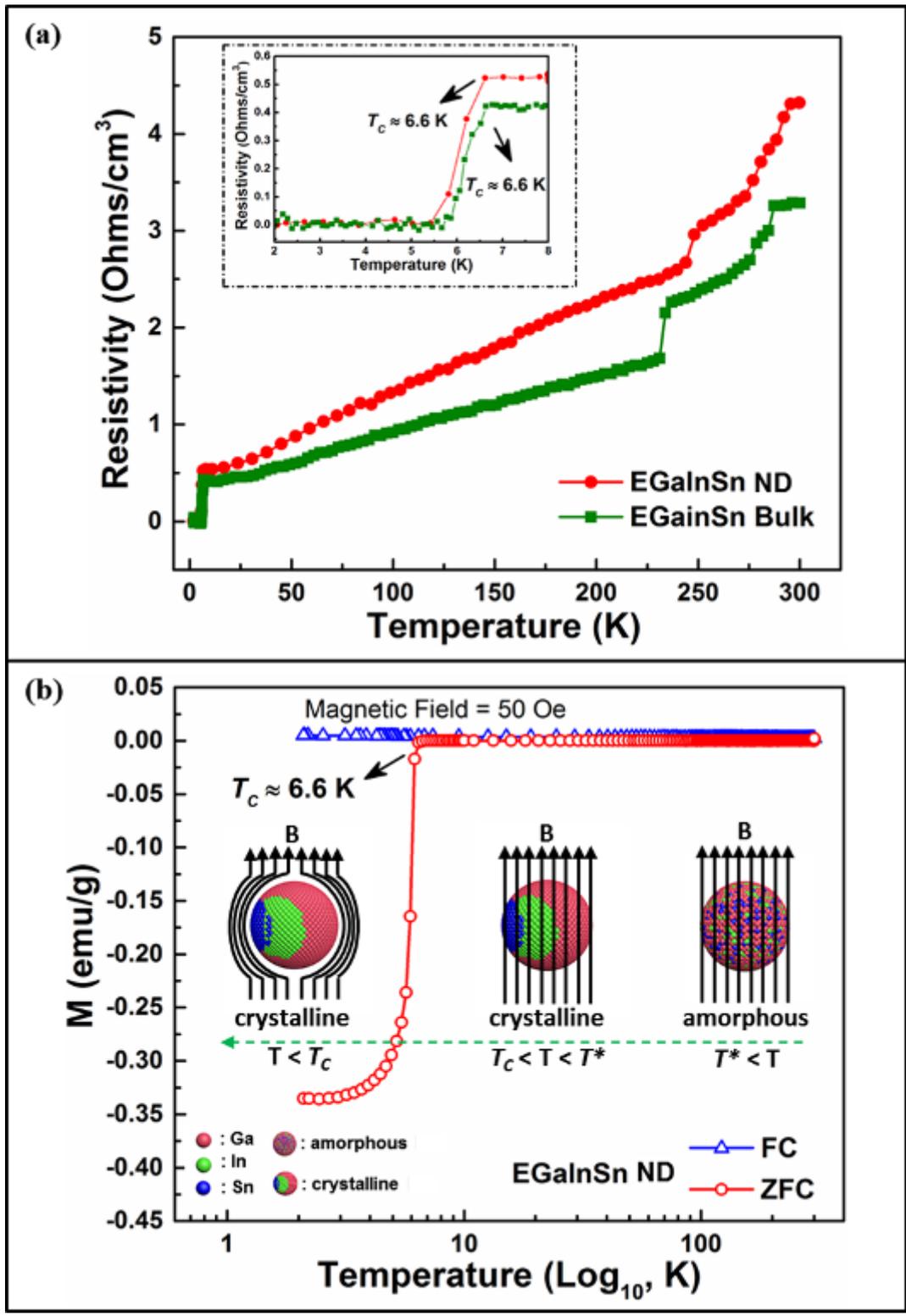
1
2
3

1 **Superconducting EGaInSn alloys and their nanosized droplets** with different weight ratios
2 have been developed for realizing printable and stretchable superconducting circuits. The
3 highest superconducting T_c of EGaInSn can reach as high as 6.6 K. The corresponding
4 EGaInSn nanodropletss retain the bulk superconducting properties and their dispersion in
5 various solvents shows excellent wettability, which can be easily used for printing stretchable
6 and flexible superconductive micro/nano electronics.
7
10
11 L. Ren, J.C. Zhuang, G. Casillas, H.F. Feng, Y.Q. Liu, X. Xu,* Y.D. Liu, J. Chen, Y. Du,* L.
12 Jiang, and S.X. Dou
13
14 **Nano-droplets for Stretchable Superconducting Circuits**
15
16

17
18
19
20